

Red Fluorescent Aminoferrrocene (Pro)Drugs for *in Cellulo* and *in Vivo* Imaging

Svitlana Chernii⁺,^[a, b] Roman Selin⁺,^[a, c] Galyna Bila,^[d, e] Rostyslav Bilyy,^[d, e] Marlies Körber,^[a] and Andriy Mokhir^{*[a]}

Red fluorescent dyes are usually charged, lipophilic molecules with relatively high molecular weight, which tend to localize in specific intracellular locations, e.g., a cyanine dye Cy5 is biased towards mitochondria. They are often used as markers of biomolecules including nucleic acids and proteins. Since the molecular weight of the dyes is much smaller than that of the biomolecules, the labelling has a negligible effect on the properties of the biomolecules. In contrast, conjugation of the dyes to low molecular weight (pro)drugs can dramatically alter their properties. For example, conjugates of Cy5 with lysosome-targeting aminoferrrocenes accumulate in mitochondria and exhibit no intracellular effects characteristic for the parent

(pro)drugs. Herein we tested several neutral and negatively charged dyes for labelling lysosome-targeting aminoferrrocenes **7** and **8** as well as a non-targeted control **3**. We found that a BODIPY derivative BDP-TR exhibits the desired unbiased properties: the conjugation does not disturb the intracellular localization of the (pro)drugs, their mode of action, and cancer cell specificity. We used the conjugates to clarify the mechanism of action of the aminoferrrocenes. In particular, we identified new intermediates, explained why lysosome-targeting aminoferrrocenes are more potent than their non-targeted counterparts, and evaluated their distribution *in vivo*.

Introduction

Metal-containing drugs play an important role in the chemotherapy of cancer diseases. They include cisplatin, oxaliplatin, and carboplatin, all of which target intracellular DNA thereby inhibiting cell proliferation. Since cancer cells usually rely on proliferation stronger than normal cells, these metallodrugs affect the former cells preferably.^[1] Since the clinically approved Pt-drugs exhibit important side effects, e.g. the pronounced toxicity towards some healthy tissues as well as the development of resistance as a result of repeated treatments,^[2] the

search for alternative solutions is actively pursued. For example, a number of potentially less toxic metallodrugs based on 3d metal ions have been developed as outlined in recent reviews.^[3–5] Among them, ferrocene-derivatives are especially prominent due to their high stability, low toxicity, facile chemical modification, and intrinsic redox properties enabling the transfer of electrons to endogenous substrates.^[6–9] For example, our group has introduced a series of ferrocene derivatives producing reactive oxygen species (ROS=H₂O₂, O₂^{•-}, HO[•]) in cancer cells. They include (a) H₂O₂-activated N-alkylaminoferrrocene-based prodrugs targeting either mitochondria^[10–12] or endoplasmic reticulum^[13] or lysosomes,^[14] (b) electronically coupled oligoferrrocene-drugs,^[15] c) lysosome-targeting aminoferrrocene drugs^[16] and d) hybrid prodrugs of known drugs, whose activity is controlled by a H₂O₂-responsive, aminoferrrocene-switch.^[17–19] The majority of these (pro)drugs are either intrinsically non-fluorescent or fluoresce in the spectral range of 300–550 nm.^[10–19] The latter signal overlaps with the cellular autofluorescence.^[20] These factors complicate the studies of uptake, intracellular distribution, and activation of the (pro)drugs *in vitro* and make such studies impossible *in vivo*.

To address this issue we have previously explored two approaches (Scheme 1). First, we labelled a representative aminoferrrocene prodrug **1** with [¹⁸F]fluoro-β-glucopyranosyl tracer to obtain conjugate **2** that we used to evaluate stability and distribution of aminoferrrocene prodrugs *in vivo* by positron emission tomography (PET).^[21] The duration of the monitoring in the latter experiment was limited to <110 min due to the short lifetime of the ¹⁸F tracer. Second, we labelled prodrug **3** and drug **4** with a red-fluorescing Cy5 dye to obtain conjugates **5** and **6**, correspondingly.^[22] The distribution of the latter conjugates *in vivo* could be conveniently observed by using the imaging system IVIS®. In contrast to the previous approach

[a] S. Chernii,⁺ R. Selin,⁺ M. Körber, A. Mokhir
Friedrich-Alexander University (FAU) of Erlangen-Nürnberg, Department of Chemistry and Pharmacy, Chair Organic Chemistry II, Nikolaus-Fiebiger str. 10, 91058 Erlangen, Germany
E-mail: Andriy.Mokhir@fau.de

[b] S. Chernii⁺
Innovation Development Center ABN LLC Pirogov str. 2/37, 01030 Kyiv, Ukraine

[c] R. Selin⁺
Institute of General and Inorganic Chemistry NASU, 32/34 Palladin Ave., 03142, Kyiv, Ukraine

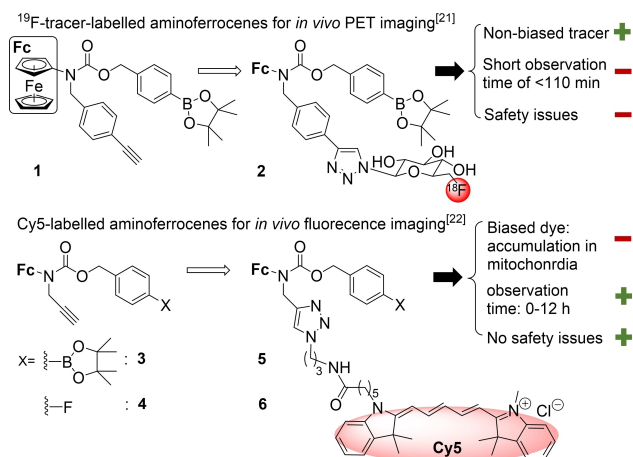
[d] G. Bila, R. Bilyy
Lectinotest R&D, Mechanichna str. 2, 79024 Lviv, Ukraine

[e] G. Bila, R. Bilyy
Danylo Halytsky Lviv National Medical University, Department of Histology, Cytology and Embryology, Pekarska str. 68, 79010 Lviv, Ukraine

[⁺] These authors contributed equally.

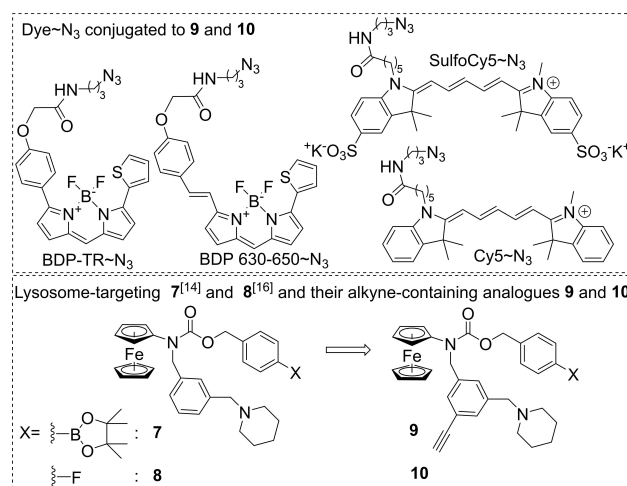
Supporting information for this article is available on the WWW under <https://doi.org/10.1002/chem.202401107>

© 2024 The Authors. Chemistry - A European Journal published by Wiley-VCH GmbH. This is an open access article under the terms of the Creative Commons Attribution Non-Commercial NoDerivs License, which permits use and distribution in any medium, provided the original work is properly cited, the use is non-commercial and no modifications or adaptations are made.



Scheme 1. Known examples of aminoferrocene-prodrugs, whose *in vivo* distribution was previously studied. “+” indicates a desired property and “-” indicates an unfavourable property.

including the use of the radioactive ^{19}F tracer, the fluorescence monitoring does not require any radioactive reagents. A further advantage is the extended over 24 h observation window due to the higher stability of Cy5 than ^{19}F . This allowed studying the relatively slow activation of aminoferrocene prodrugs *in vivo*. Unfortunately, the (pro)drug~Cy5 conjugates exhibited a very strong bias towards accumulation in the mitochondria of cells. Similar behavior has been previously observed by research groups of Mailänder and Bao for a variety of Cy5~oligonucleotide conjugates.^[23,24] These data allow concluding that the use of Cy5 and related dyes are restricted to mitochondria-targeting (pro)drugs, whereas labelling of non-targeting or targeting other organelles (pro)drugs (e.g., ER^[13] and lysosomes^[14]) can lead to wrong conclusions. Therefore, the search for non-biased, red fluorescing dyes suitable for labelling of low molecular weight (pro)drugs and compatible with *in vivo* imaging is warranted.^[25] Herein, we report on the synthesis and characterization of conjugates of potentially non-biased dyes (sulfoCy5, BODIPY derivatives BDP-TR and BDP 630–650, Scheme 2) as well as the control biased dye Cy5 with representative lysosome-targeting aminoferrocene prodrug **7**^[14] and drug **8**^[16] (Scheme 1) as well as a non-targeting control **3** (Scheme 1). We confirmed that the best conjugates in this series (**15**, **16**) induce analogous to the parent (pro)drug cell phenotypes including similar patterns of intracellular accumulation and ROS generation. We used these conjugates to investigate for the first time the activation of lysosome-targeting aminoferrocene (pro)drugs in representative cancer cells (human ovarian cancer A2780 cells) by using LC-MS and their accumulation in different tissues in mice bearing solid Nemeth-Kellner (NK) lymphoma (Ly).



Scheme 2. Structures of selected dye derivatives and (pro)drugs for the synthesis of (pro)drug~dye conjugates.

Results and Discussion

Selection of Red Fluorescing Dyes and Model (Pro)Drugs

Based on its structure and literature data,^[23,24,26] Cy5 can be classified as delocalized lipophilic cation (DLC). Its binding to the negatively charged membrane of mitochondria depends on the presence of the delocalized positive charge. We assumed that neutral or negatively charged dyes would not interact with the mitochondrial membrane and, therefore, remain unbiased.^[25] To test this hypothesis, we selected BODIPY dyes BDP TR ($\lambda_{\text{ex}} = 589 \text{ nm}$, $\lambda_{\text{em}} = 616 \text{ nm}$) and BDP 630–650 ($\lambda_{\text{ex}} = 628 \text{ nm}$, $\lambda_{\text{em}} = 642 \text{ nm}$) as representative red fluorescing neutral dyes and a cyanine dye sulfoCy5 ($\lambda_{\text{ex}} = 646 \text{ nm}$, $\lambda_{\text{em}} = 662 \text{ nm}$) as a representative red fluorescing negatively charged dye (Scheme 2). All these dyes are commercially available as azides (Lumiprobe, Hannover, DE). We used lysosome-targeting aminoferrocene prodrug **7**^[14] and drug **8**^[16] as models for testing the bias of the dyes toward mitochondria. Specifically, (pro)drug~dye conjugates with nonbiased dyes will accumulate in lysosomes similarly to the parent (pro)drugs (desired effect). In contrast, (pro)drug~dye conjugates with biased dyes will accumulate in mitochondria (undesired effect). Further, the availability of red fluorescing derivatives of **7** and **8** could help in clarification of the mode of action of these promising (pro)drugs *in cellulo* and *in vivo*, for which, currently only scarce data are available.^[14,16]

Synthesis of (Pro)Drug~Dye Conjugates

For the conjugation of **7** and **8** to the selected dyes, we have introduced an alkyne moiety to their structures to obtain **9** and **10** correspondingly. These intermediates were prepared as previously reported.^[16] Coupling of **9**, **10**, and control **3** to the selected dye~N₃ intermediates (Scheme 2) via the Cu(I)-catalyzed alkyne-azide cycloaddition (CuAAC) furnished the con-

jugates **11–18** with moderate to good yields of 32–65% (Table 1, supporting information, *SI*).

The identity of the products was confirmed by either high-resolution electrospray or atmospheric pressure photochemical ionization mass spectrometry (HR-ESI-MS or HR-APPI-MS). In particular, differences between found and calculated mass-to-charge ratios (m/z) for molecular ions were in all cases less than 3 ppm (Table 1). The purities of the conjugates were > 95%, except that of conjugate **13** (> 90%), as confirmed by HPLC coupled to UV- and MS detectors (*SI*).

Validation of the Applicability of the Selected Dyes for Labelling of Aminoferroccene (Pro)Drugs

Fluorescent Properties of the Conjugates

All prepared conjugates strongly emit light > 600 nm (Figures 1A, B and S17, *SI*). The emission does not overlap with the cellular autofluorescence^[20] indicating that these conjugates can be imaged with high sensitivity *in cellulo* and *in vivo*. We found that the derivatives of Cy5 (**11**, **12**) and SulfoCy5 (**13**, **14**) are brighter than those of BDP-TR (**15**, **16**) and BDP 630–650 (**17**). Therefore, in most of the experiments reported in this paper, we applied the former conjugates at the concentration of 50 nM, whereas the latter ones – at 200 nM.

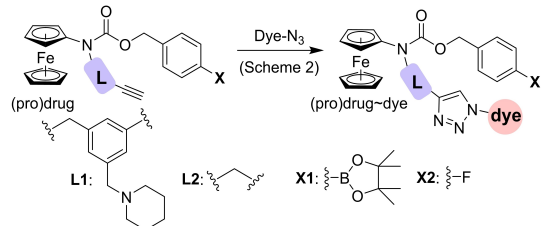
Uptake of the Conjugates and their Intracellular Localization

Since the parent prodrug **7** (IC_{50} 5.6 ± 1.7 μ M, μ M, 48 h incubation) and drug **8** (IC_{50} $= 7.0 \pm 1.3$ μ M, 48 h incubation) are toxic towards human ovarian cancer A2780 cells,^[14,16] we

selected these cells for the experiments with the fluorescently labelled conjugates of **7** (**11**, **13**, **15**, **17**) and **8** (**12**, **14**, **16**). In particular, we first evaluated the uptake of the conjugates by using fluorescence microscopy (Figures 1C–I). The cells were incubated with the conjugates for 20 min and afterward imaged by using one of two channels: Ch3 – excitation at λ_{ex} = 538–562, emission at λ_{em} 570–640 nm for detection of the derivatives of a BDP-TR dye and Ch4 – λ_{ex} = 625–655, λ_{em} 665–715 nm for detection of the derivatives of Cy5, SulfoCy5 and BDP 630–650 dyes. We found that conjugates of Cy5 (**11**, **12**), BDP-TR (**15**, **16**) and BDP 630–650 (**17**) efficiently stain A2780 cells under the chosen conditions (Figures 1C, D, G–I). In contrast, incubation of the cells with SulfoCy5-conjugates **13** and **14** does not lead to the increase of the intracellular fluorescence characteristic for the SulfoCy5 dye (Ch4). Extending the incubation from 20 to 120 min does not improve the uptake of **13** and **14** (Figures S18C and D, *SI*). These data indicate that the conjugates **13** and **14** are practically not cell membrane permeable (Figures 1E and F). Correspondingly, SulfoCy5 is not a suitable dye for labelling aminoferroccene (pro)drugs usually affecting intracellular targets.^[14,16] Though the BDP 630–650 conjugate **17** is uptaken by A2780 cells (Figures 1I, 18G, *SI*), we did not pursue its evaluation, since stock solutions of **17** were found to be unstable. In particular, its concentration was continuously reduced with time, even when stored at -23 °C. All other experiments were conducted with the conjugates of BDP-TR, whereas the conjugates of Cy5 were used as biased to mitochondria controls.^[22]

We found that the emission of the conjugate of prodrug **7** with Cy5 (**11**) colocalizes with that of the mitochondria-specific dye MitoTracker GreenTM (Pearson's coefficient $r = 0.87 \pm 0.05$, Figures 2A–D). In contrast, its parent, unlabeled prodrug **7** is known to localize in the lysosomes of the cells.^[14] Thus, the properties of the conjugate **11** are defined by the dye (Cy5) rather than the prodrug (aminoferroccene **7**). Analogous results were obtained for the conjugate of lysosome targeting drug **8** and Cy5 (**12**, Figure S21B). These data confirm our previous findings that Cy5 is a strongly mitochondria-biased dye, which is not suitable for labelling drugs targeting other than mitochondria organelles.^[22] The replacement of the positively charged Cy5 with the neutral BDP-TR gave rise to the conjugate **15**. Emission of this conjugate loaded to A2780 cells co-localizes with that of the lysosome-specific dye LysoTracker GreenTM ($r = 0.83 \pm 0.08$, Figures 2E–H). Analogous results were obtained for the conjugate of lysosome targeting drug **8** and BDP-TR (**16**, Figure S21C). These data indicate the lysosomal localization of **15** and **16** which is the same localization pattern as previously observed for the unlabeled **7**^[14] and **8**.^[16] The latter conclusion was confirmed for conjugate **15** by confocal microscopy (Figure S21D, *SI*). Furthermore, we found that the conjugate of prodrug **3** and BDP-TR (**18**) does not accumulate to a substantial degree in lysosomes ($r = 0.49 \pm 0.07$), exhibit some preference for mitochondria ($r = 0.69 \pm 0.11$, Figures S21A and B, *SI*) and does not accumulate in nuclei of A2780 cells (Figure S18H, *SI*). This is similar to the expected localization pattern of the unlabeled **3**.^[27] Thus, the conjugates of non-mitochondria-targeting aminoferroccenes with the BDP-TR dye

Table 1. A numbering scheme and identification data for synthesized (pro)drug~dye conjugates.



L/X ^[a]	Dye ^[a]	Conjugate	m/z , calcd ^[b]	m/z , found
L1/X1	Cy5	11	1237.6486	1237.6485
L1/X2	Cy5	12	1129.5555	1129.5557
L1/X1	SulfoCy5	13	1397.5621	1397.5655
L1/X2	SulfoCy5	14	1289.4663	1289.4687
L1/X1	BDP-TR	15	1179.4423	1179.4378
L1/X2	BDP-TR	16	1071.3467	1071.3425
L1/X1	BDP 630–650	17	1205.4580	1205.4597
L2/X1	BDP-TR	18	1005.3128	1005.3137

[a] See Scheme 2 for structures of the dyes. [b] Brutto formulae are provided in the *SI*.

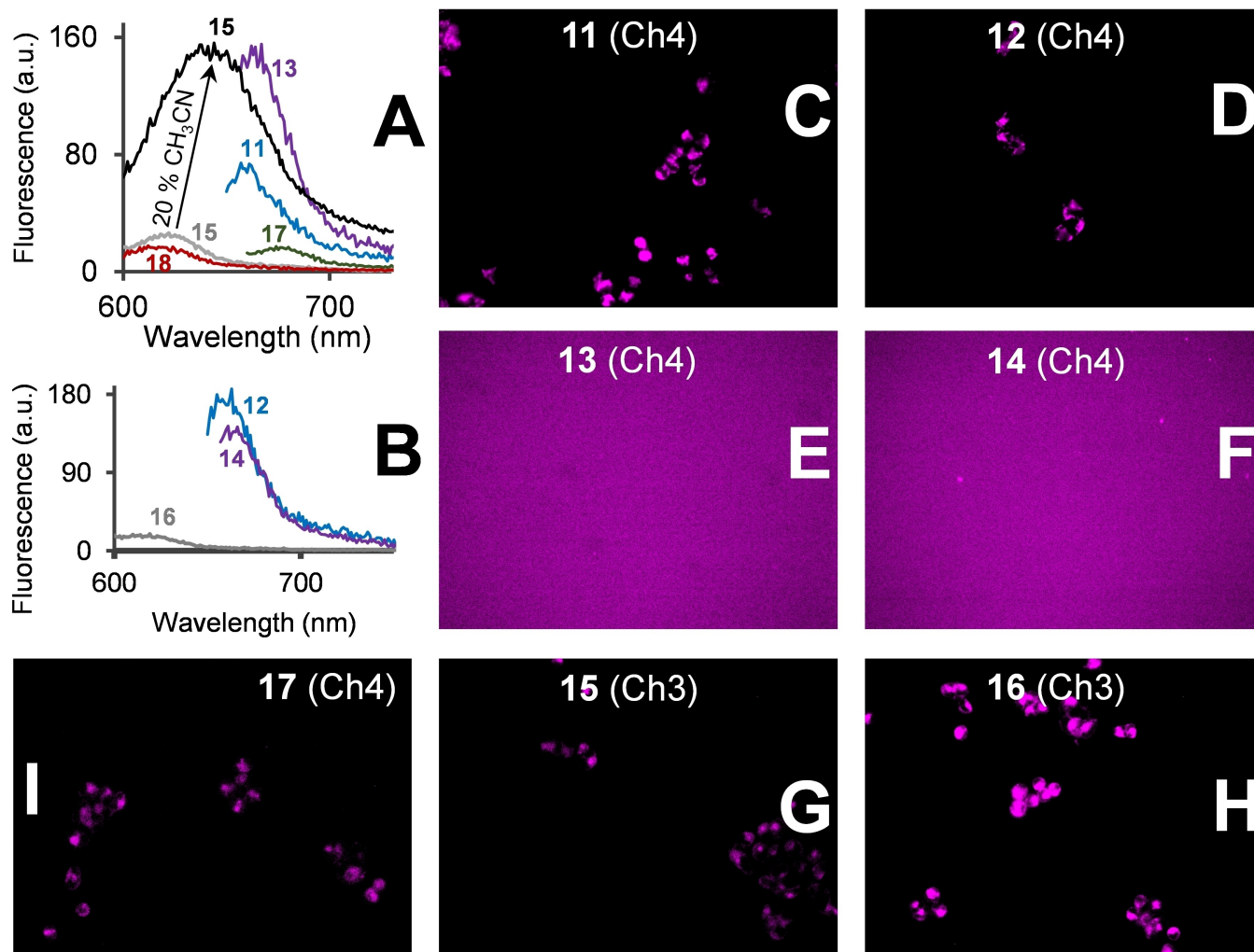


Figure 1. A, B: Fluorescence spectra of conjugates 11, 13 (both 50 nM), 15 (with and without 20% CH₃CN, v/v), 17 (both 200 nM) (A) as well as 12, 14 (both 50 nM), 16, 17 (both 200 nM) in phosphate-buffered saline containing DMSO (0.01%, v/v). Excitation λ_{ex} = 640 nm (11, 12); 647 nm (13, 14); 590 nm (15, 16); 620 nm (17); 580 nm (18). C–I: Fluorescence microscopy images of A2780 cells incubated with the corresponding conjugates for 20 min. Ch3 = Channel 3: λ_{ex} = 538–562; λ_{em} 570–640 nm; Ch4 = Channel 4: λ_{ex} 625–655/ λ_{em} 665–715 nm. Detailed experimental conditions and additional images are provided in Figure S18, SI.

accumulate at the same intracellular locations as unlabeled aminoferrocenes as confirmed for three cases: 15, 16, and 18.

As previously established, the prodrug 7 and the drug 8 exhibit distinct modes of action by affecting different pools of intracellular ROS in cancer cells. In particular, the prodrug 7 increases the level of total ROS (tROS) as determined by using 5-(6-chloromethyl-2',7'-dichlorodihydrofluorescein diacetate probe (CM-DCFH-DA),^[14] whereas the drug 8 facilitates the production of mitochondrial ROS (mROS) as determined by using MitoSOXTM probe.^[16] We were pleased to observe that the fluorogenic versions of these (pro)drugs 15 and 16 behave similarly (Figures 3A and B).

Furthermore, drug 8 is known to increase mROS only in cancer cells (e.g. A2780), whereas healthy cells (e.g., SBLF9) remain unaffected.^[16] This effect could also be reproduced by using the fluorescent version of 8 (16) (Figure S23, SI). Thus, the data from this section indicate that BDP-TR is a non-biased dye that affects neither the intracellular localization of (pro)drugs

nor their mode of action nor their cancer cell specificity. This makes BDP-TR especially useful for fluorescent labelling of low molecular weight (pro)drugs for *in cellulo* and *in vivo* applications.

Applications of the BDP-TR-Labelled Conjugates

Chemistry of Intracellular Transformations of 15 and 16

Further, we used the fluorescent analogues of 7 (15) and 8 (16) to study for the first time the intracellular transformations of the lysosome-targeting aminoferrocene (pro)drugs. To get the reference data, we studied the stability of both conjugates in aqueous solutions in the absence and presence of H₂O₂ to model the situation they encounter in cancer cells with higher ROS levels than healthy cells. In the absence of H₂O₂, 95% of conjugate 15 (retention time (R_t) = 11.7 min, observed m/z

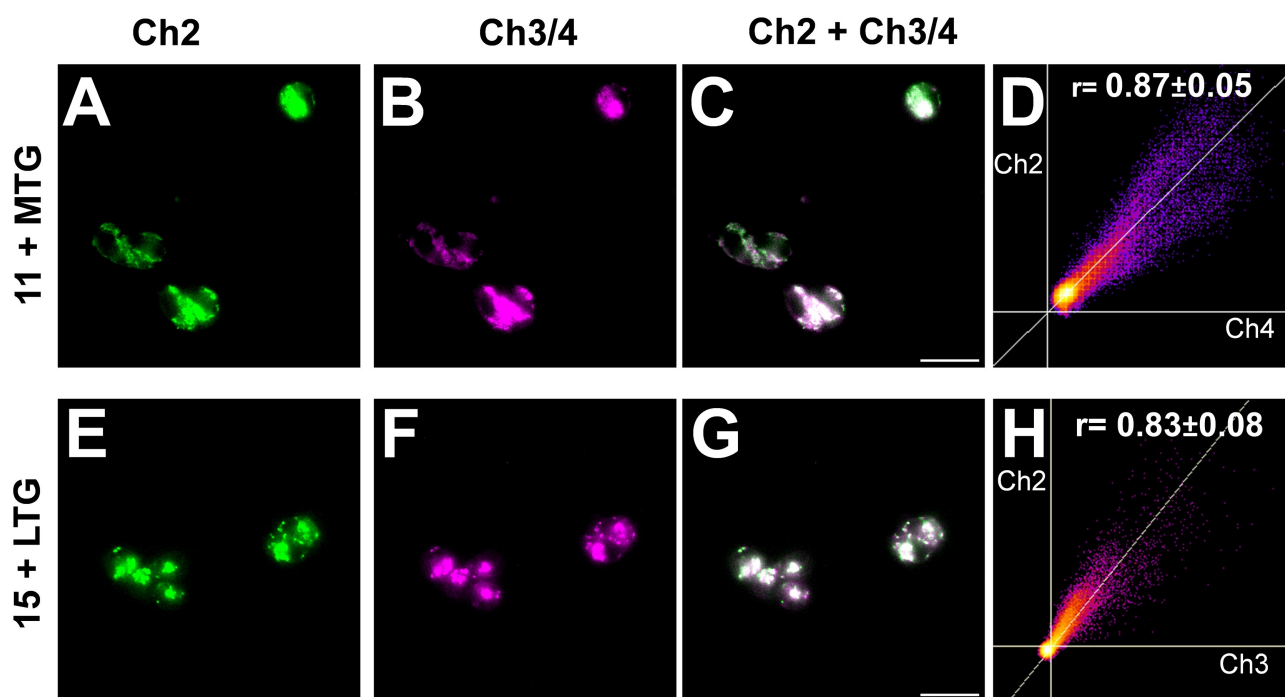


Figure 2. Identification of intracellular localization of the conjugates in A2780 cells. **A–D:** Co-localization of **11** (200 nM) with MitoTracker™ Green (MTG, 100 nM). **E–H:** Co-localization of **15** (200 nM) with LysoTracker™ Green (LTG, 50 nM). Co-localization coefficients R_{coloc} were calculated using ImageJ and shown as frequency diagrams and r values. Ch2 (green): λ_{ex} 450–490, λ_{em} 500–550 nm. Ch3 (magenta): λ_{ex} 538–562, λ_{em} 570–640 nm for **15**. Ch4 (magenta): λ_{ex} 625–655, λ_{em} 665–715 nm for **11**. Scale bar – 10 μm .

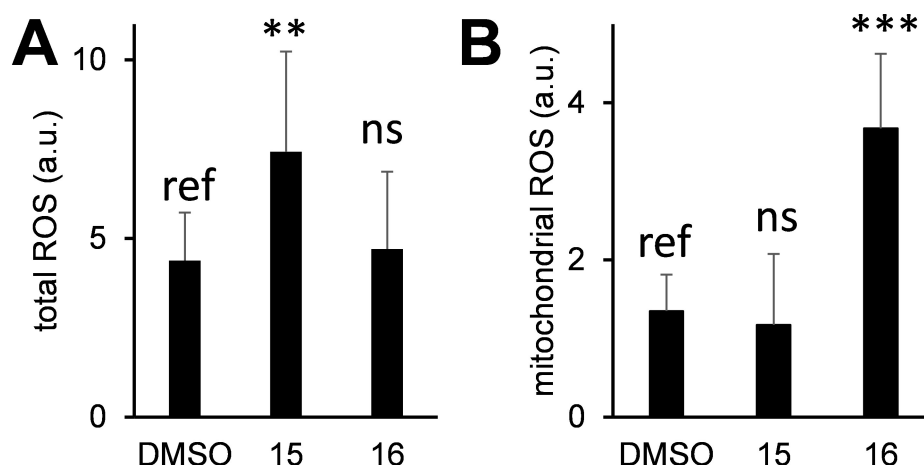
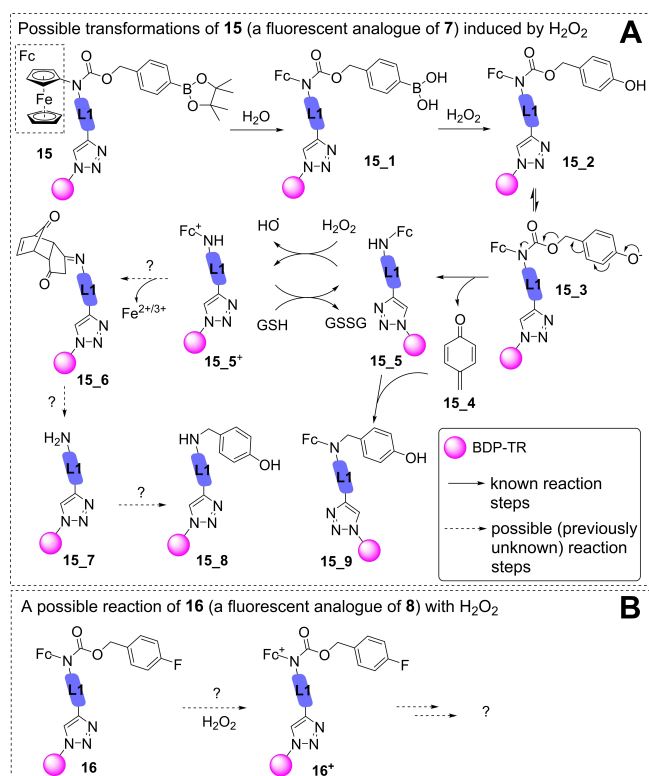


Figure 3. Effect of conjugates **15** and **16** on the levels of intracellular total ROS and mitochondrial ROS in A2780 cells. Control probe (“DMSO”) was used as a reference in statistical Students t -test: ** – $p < 0.01$; *** – $p < 0.001$; ns – non-significant ($p > 0.05$). Other experimental details are provided in the *SI*. Error bars correspond to standard deviations of the mean values determined from at least 3 independent experiments ($N \geq 3$).

1179 Da, $[\text{M} + \text{H}^+]^+$) is hydrolyzed within 24 h with the formation of boronic acid **15_1** ($R_t = 10.5$ min, m/z 1097 Da, $[\text{M} + \text{H}^+]^+$) (Scheme 3, Figure S25A). The same result was obtained in the presence of either glutathione (5 mM) or bovine serum albumin (0.1 mg/mL) (Figures S25B and C, *SI*). In the presence of H_2O_2 , the boronic acid **15_1** is further converted to phenol **15_2** ($R_t = 11.9$ min, m/z 1069 Da, $[\text{M} + \text{H}^+]^+$) in the B–C–bond cleavage reaction (Figure 4A).

The phenol exists in equilibrium ($\text{pK}_a \sim 10$) with its phenolate **15_3**, which irreversibly and spontaneously decomposes to

para-quinone methide **15_4** (not detected in the LC-UV-MS trace), aminoferrocene **15_5** ($R_t = 11.9$ min, m/z 918 Da, $[\text{H} - \text{e}^-]^+$) and its oxidized form **15_5^+** ($R_t = 6.8$ min, m/z 918 Da, $[\text{H} - \text{e}^-]^+$) in the result of the sequential 1,6-elimination, CO_2 release, and oxidation reaction. Though para-quinone methide is not directly detectable, its formation could be indirectly confirmed. In particular, we observed intermediate **15_9** ($R_t = 10.7$ min, m/z 1024 Da: $[\text{M} - \text{e}^-]^+$) and its oxidized form **15_9^+** ($R_t = 6.8$ min, m/z 1024 Da: $[\text{M} - \text{e}^-]^+$) resulting from the *in situ* alkylation of the aminoferrocene **15_5** by the **15_4**. All these intermediates were



Scheme 3. Possible mechanisms of reactions of fluorescent prodrug **15** (A) and drug **16** with H_2O_2 (B) based on the data reported for unlabelled parent prodrug **7**^[14] and drug **8**^[16]

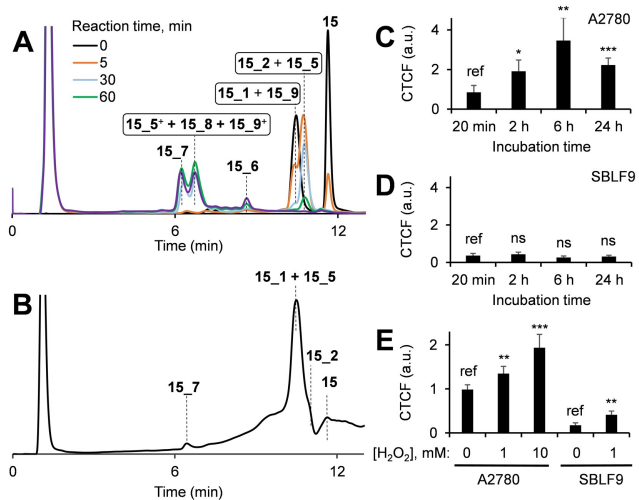


Figure 4. Monitoring the reaction of **15** with H_2O_2 in cell-free settings (A) and within A2780 cells (24 h incubation, B) by using HPLC. Y axis: light absorbance at 254 nm. The fractions were identified by mass spectrometry. Experimental details are provided in the *SI*. C, D: Quantifications of changes of the intracellular fluorescence of either A2780 (C) or SBLF9 cells (D) loaded with conjugate **15** for 20 min, washed and further incubated for up to 24 h by calculating the corrected total cell fluorescence (CTCF, Ch3: $\lambda_{\text{ex}} = 538\text{--}562$; $\lambda_{\text{em}} = 570\text{--}640$ nm) from microscopy images shown in Figures S28, S29, *SI*. E: The same as C and D, except that the cells were loaded with **15** (20 min), followed by incubation with the shown H_2O_2 concentrations for 2 h. The corresponding fluorescence images are shown in Figure S30, *SI*. The data were compared by using statistical Student's *t*-test; a reference is indicated with "ref": * - $p < 0.05$, ** - $p < 0.01$, *** - $p < 0.001$; ns - non-significant ($p > 0.05$). Error bars correspond to standard deviations of the mean values determined from at least 3 independent experiments ($N \geq 3$).

previously described for the H_2O_2 -induced activation of the parent prodrug **7**.^[12] Additionally to the known intermediates, we detected **15_6** ($R_t = 8.7$ min, m/z 893 Da: $[\text{M} + \text{H}^+]^+$), which is the product of decomposition of aminoferrocene **15_5**, followed by 2+4 cycloaddition of cyclopentadiene (the lower Cp in the **15_5**, Scheme 3) with substituted cyclopentadiene (the upper Cp in the **15_5**) and the final oxidation. It is also possible that the Cp's are first oxidized and then undergo 2+4 cycloaddition. The intermediate **15_5** is an imine, which is expected to be hydrolytically unstable in water. In agreement with this expectation, we detected the hydrolysis product of **15_5**, amine **15_7** at $R_t = 6.2$ min (m/z 735 Da: $[\text{M} + \text{H}^+]^+$). Furthermore, the product of the amine alkylation by para-quinone methide **15_4** (**15_8**) was observed at $R_t = 6.8$ min (m/z 841 Da: $[\text{M} + \text{H}^+]^+$) correspondingly.

After over 2 h incubation of **15** and H_2O_2 two stable organic compounds **15_7** (major) and **15_8** (minor) are formed. All other intermediates described above are unstable (Figure 4A). We managed to isolate the former product in its pure form by using HPLC (Figure S27, *SI*). This compound was used as a reference in studies of the transformation of **15** in A2780 cells. In this experiment, representative cancer A2780 cells were loaded with **15** (5 μM) for 2 h, washed and incubated for 24 h that was followed by further washing and cell lysis. The mixture obtained was analyzed by LC-UV-MS using the protocol described in the *SI*. We detected the initial prodrug **15** as traces, whereas the hydrolyzed prodrug **15_1** was present in the substantial amount (Figure 4B). Furthermore, intermediates phenol **15_2** and aminoferrocene **15_5** as well as the stable product, amine **15_7** were also observed. These data confirm for the first time that the H_2O_2 -induced intracellular transformation of **15** occurs in cells according to the mechanism outlined in Scheme 3. This experiment also indicates that the intracellular activation of **15** is low-yielding after 24 h incubation.

In contrast to **15**, conjugate **16** was found to be stable in the presence of H_2O_2 both in cell-free settings and in A2780 cells after 24 h incubation (Figure S26, *SI*) which is in agreement with the previous data for the unlabelled parent drug **8**.^[16]

Kinetics of Activation of Aminoferrocene (Pro)Drugs in Representative Cancer A2780 and Healthy SBLF9 Cells

We selected for this study fluorogenic lysosome targeting prodrug **15**, lysosome targeting drug **16**, and non-targeting prodrug **18** as a control. The conjugate **15** dissolved in the aqueous buffer (phosphate 10 mM, pH 7.5, NaCl 150 mM, GSH 5 mM) containing DMSO (0.05%, v/v) fluoresces weakly: $\lambda_{\text{ex}} = 590$ nm, $\lambda_{\text{em}} = 20$ nm, fluorescent quantum yield $\varphi_{\text{fluo}}(\mathbf{15}) = 0.6\%$ (*SI*). The addition of CH_3CN (20%, v/v) to the solution of **15** leads to an 11-fold fluorescence increase (Figure 1A). These data indicate that the fluorescence quenching can be caused by aggregation of **15** in solution. We confirmed this possibility by using dynamic light scattering (DLS). In particular, we detected nanoparticles with a mean diameter of 85 ± 4 nm in the aqueous solution of conjugate **15**, whereas these were not

present in the solution of **15** in CH₃CN. In contrast to **15**, the product formed in its reaction with H₂O₂, amine **15_7** (Scheme 3, Figure 4A) is strongly fluorescent: $\varphi_{\text{fluo}}(\mathbf{15_7})=81\%$. The ratio of fluorescent quantum yields of **15_7** and **15** is equal to 135, which is the maximal fluorescence increase expected in the reaction of **15** with H₂O₂.

We used the favorable fluorogenic properties of conjugate **15** to investigate the kinetics of its activation in cells. First, we incubated representative cancer A2780 cells, which contain elevated levels of H₂O₂,^[14] with **15** (100 nM) for 20 min and washed the cells to remove the excess of **15**. The cells were imaged either immediately after that or after 2, 6, and 24 h incubation. We found that the cell emission characteristic for **15** and the derived from **15** products is increased from 20 min to 6 h incubation, whereas it is slightly decreased after 24 h incubation. These data indicate that **15** is activated in the cancer cells with the formation of fluorescent products. According to our LC-UV-MS data (Figure 4B), these products are aminoferrocene **15_5** and amine **15_7**. In contrast, conjugate **15** is not activated in healthy SBLF9 cells (Figure 4D), which do not contain H₂O₂.^[14] The same result was obtained when **15** was incubated with co-cultured A2780 and SBLF9 cells (Figure S31, S1). The addition of H₂O₂ (1 mM) to SBLF9 cells loaded with **15** leads to the fluorescence increase (Student's t-test, $p < 0.01$, Figure 4E). The same effect is also observed for A2780 cells loaded with **15**. These data further confirm that the prodrugs are activated in cells in the reaction with H₂O₂.

In contrast to **15**, the fluorescence of A2780 cells loaded with conjugate **16** is substantially lower at all tested incubation times: 6.1–14.6 fold (Figures 4C, S28, S31, S33). These data confirm that **16** is not converted to any metabolite in cells which is the expected result based on the previous data reported for the non-labelled, parent drug **8**.^[16]

We observed an interesting effect in a similar experiment conducted with the control conjugate **18**, which is a labelled analogue of non-targeted prodrug **3**. In particular, A2780 cells loaded with **18** exhibits substantial fluorescence at the shortest tested incubation time of 20 min (the fluorescence intensity is 1.8 fold higher than that of the cells loaded with **16**, Figures S32–S34) indicating the intracellular activation of the prodrug. In contrast, at the 2–24 h incubation, the fluorescence of the cells loaded with **18** is 2-fold lower than that of the cells loaded with **16**. These data may indicate that the drug initially formed from **18** is deactivated or eliminated from the cells that neutralizes the effect of the drug. The drug deactivation/elimination is not observed for the lysosome targeted **15**. This effect explains the higher anticancer activity of prodrug **7** (the parent prodrug of **15**)^[14] than that of **3** (the parent prodrug of **18**).^[27]

Distribution of Conjugates **15** and **16** in Organs of Mice Carrying Nemeth-Kellner Lymphoma

To investigate the distribution and activation of conjugates **15** and **16** *in vivo*, we selected murine Nemeth-Kellner lymphoma subclone RB (NK/Ly-RB). These cells were implanted in mice of

Balb/c type, where they grew as well-defined solid tumors. According to our previous studies these tumors produce higher levels of ROS than normal tissues. Aminoferrocene prodrugs exhibit potent antitumor activity in this model.^[14,16,17]

Both conjugates **15** and **16** were applied via intraperitoneal (i.p.) injections at the doses of 1 nmol per mouse, incubated for 24 h, and the distribution of the conjugates and their fluorescent intermediates were visualized (Figure 5A).

Afterward, the mice were ethically sacrificed, their organs isolated and the fluorescence of the organs quantified (Figure 5B). In both cases the emission was detected at two channels: $\lambda_{\text{ex}}=685\text{ nm}$, $\lambda_{\text{em}}=700\text{ nm}$ (indicated as green color) and $\lambda_{\text{ex}}=785\text{ nm}$, $\lambda_{\text{em}}=800\text{ nm}$ (indicated as red color) by using LiCor Pearl IR imager. The first channel was selected since it partially overlaps with the optical properties of conjugates **15**, **16** and the products of their reaction with H₂O₂ (Figures 1A and B). The second channel was selected as a control since the latter compounds were not expected to be fluorescent in this area.

The fluorescence in organs of the gastrointestinal tract (stomach, duodenum, and cecum, green channel) can be caused by fluorescent plant derivatives in the food of mice. This signal was not further considered. Otherwise, we found a substantial accumulation of the fluorescence signal (green channel) derived from prodrug **15** and drug **16** in tumors, kidney, and the liver. Interestingly, **16** also gives rise to a significant signal in the lung and inguinal lymph node, whereas the **15**-derived signals in these organs are weaker. This observation is in agreement with the better tolerability of

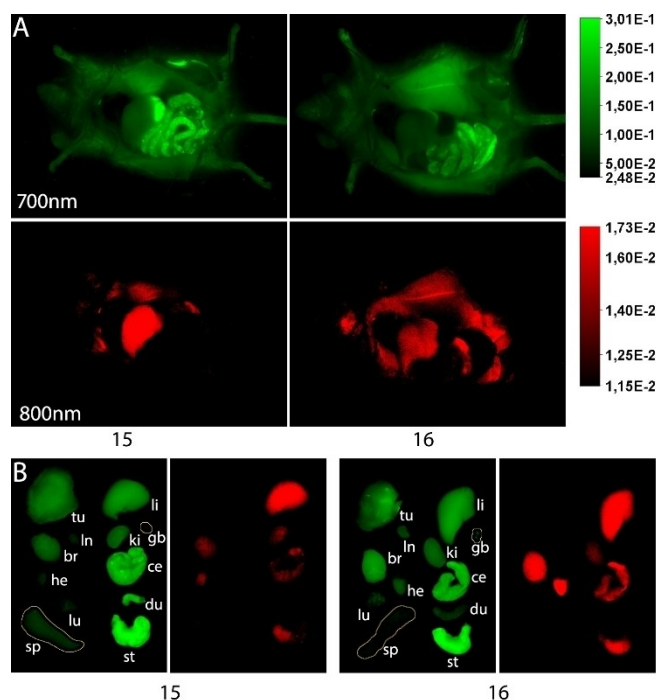


Figure 5. Fluorescence imaging of NK/Ly-RB mice treated with conjugates **15** and **16**. Fluorescence emission at 700 nm was visualized green, at 800 nm – red. **A:** Mice imaged after 24 h incubation with one of the conjugates. **B:** Organs of the mice: sp – spleen, lu – lung, he – heart, br – brain, ln – inguinal lymph node, tu – tumor, st – stomach, du – duodenum, ce – cecum, ki – kidney, gb – gall bladder, li – liver.

prodrug **7**^[14] (analogue of **15**) than drug **8**^[16] (analogue of **16**). We observed that both tested aminoferrocenes accumulate to some degree in the brain, which is a previously not established fact. This may potentially be a cause of not yet identified side effects, but also can lead to new applications of the (pro)drugs for the treatment of brain diseases, e.g. brain tumor.

We were surprised to observe the substantial fluorescent signal at 800 nm (red channel) in the mice treated with the conjugates (Figure 5). These signals are derived from **15** and **16** since they are not observed in the non-treated mice. Interestingly, the 800 nm signal is not observed in tumors but detected in a few healthy organs including livers for both **15** and **16**, and in the heart and brain for **16** (Figures 5, S35, S1). We speculate that this signal can correspond to unknown metabolites of **15** and **16** formed *in vivo*. Drug **16** seems to form more of such metabolites than prodrug **15** (Figures 5 and S35, S1).

Experimental Section

Synthetic protocols for preparation of new compounds, characterization of new compounds as well as additional experimental details are provided in the Supporting Information.

Conclusions

We identified BODIPY dye BDP-TR as a red fluorescent, non-biased marker for labelling low molecular weight aminoferrocene prodrugs and drugs. The conjugation of this dye (a) does not affect the intracellular localization of the (pro)drugs, (b) their mode of action including the H₂O₂-mediated intracellular activation and the particular pattern of the release of reactive oxygen species in cancer cells, and (c) their cancer cell *versus* healthy cell specificity. We used the labelled derivatives of lysosome targeting aminoferrocenes **7** and **8** and non-targeted **3** to study their mechanism of activation in cancer cells. In particular, we identified three new products **15_6**, **15_7**, and **15_8** in the reaction of the labelled **7** (**15**) with H₂O₂ in cell-free settings and confirmed the formation of **15_5** and **15_7** in A2780 cells. Next, we found that the labelled **8** (**16**) is not decomposed in cancer cells. In contrast, we observed the quick intracellular activation of the labelled **3** (**18**) in A2780 cells which is followed by the elimination of the corresponding products from the cells. The latter data explain the low anticancer activity of **3**. The elimination of the activated intermediates was not observed for the fluorescent derivatives of a more potent anticancer prodrug **7** (**15**) and a drug **8** (**16**). Finally, we evaluated the distribution of the latter two conjugates (**15**, **16**) in Nemeth-Kellner lymphoma-carrying mice *in vivo*. The data revealed the accumulation of both **15** and **16** in tumors. The conjugate **16** accumulated stronger than **15** in healthy organs which explains the higher toxicity of **8** than that of **7**. In summary, the new data dramatically improve our knowledge of the mode of action of anticancer aminoferrocenes. Potentially, the application of BDP TR can be extended to

labelling of other than aminoferrocenes (pro)drugs that will have a substantial impact on drug discovery.

Supporting Information Summary

The authors have cited additional references within the Supporting Information.^[28–30] Synthetic protocols for preparation and characterization of new compounds as well as description of assays for studies in cell-free settings, in cells, and *in vivo*.

Acknowledgements

We thank the German Research Council (DFG, MO 1418/7-2) and European Union (grant agreement IDs: 872331 – NoBias-Fluors, RISE program and 861878 – NeuroCure, FET Open program) for funding this project. RS thanks Alexander von Humboldt Foundation – Philipp Schwartz Initiative and SC – Federation of European Biochemical Societies (FEBS) for providing individual fellowships. Open Access funding enabled and organized by Projekt DEAL.

Conflict of Interests

The authors declare no conflict of interest.

Data Availability Statement

The data that support the findings of this study are available in the supplementary material of this article.

Keywords: Red fluorescent dye · Prodrug · Drug · Imaging · Cancer

- [1] C. Zhang, C. Xu, X. Gao, Q. Yao, *Theranostics* **2022**, *12*, 2115.
- [2] R. Oun, Y. E. Moussa, N. J. Wheate, *Dalton Trans.* **2018**, *47*, 6635.
- [3] M. M. González-Ballesteros, C. Mejia, L. Ruiz-Azuara, *FEBS Open Bio* **2022**, *12*, 880.
- [4] Q. Peña, A. Wang, O. Zaremba, Y. Shi, H. W. Scheeren, J. M. Metselaar, F. Kiessling, R. M. Pallares, S. Wuttke, T. Lammers, *Chem. Soc. Rev.* **2022**, *51*, 2544.
- [5] A. Casini, A. Pöthig, *ACS Central Science* **2024**. DOI: 10.1021/acscentsci.3c01340.
- [6] R. Das, D. R. Chatterjee, A. Shard, *Coord. Chem. Rev.* **2024**, *504*, 215666.
- [7] H. Skoupilova, M. Bartosik, L. Sommerova, J. Pinkas, T. Vaculovic, V. Kanicky, J. Karban, R. Hrstka, *Eur. J. Pharm.* **2020**, *867*, 172825.
- [8] R. Wang, H. Chen, W. Yan, M. Zheng, T. Zhang, Y. Zhang, *Eur. J. Med. Chem.* **2020**, *190*, 112109.
- [9] A. Vassières, Y. Wang, M. J. McGlinchey, G. Jaouen, *Coord. Chem. Rev.* **2021**, *430*, 213658.
- [10] H.-G. Xu, V. Reshetnikov, M. Wondrak, L. Eckardt, L. A. Kunz-Schughart, C. Janko, R. Tietze, C. Alexiou, H. Borchardt, A. Aigner, W. Gong, M. Schmitt, L. Sellner, S. Daum, H. G. Özkan, A. Mokhir, *Cancers* **2022**, *14*, 208.
- [11] V. Reshetnikov, H. G. Özkan, S. Daum, C. Janko, C. Alexiou, C. Sauer, M. R. Heinrich, A. Mokhir, *Molecules* **2020**, *25*, 2545.
- [12] V. Reshetnikov, S. Daum, C. Janko, W. Karawacka, R. Tietze, C. Alexiou, S. Paryzhak, T. Dumych, R. Bilyy, P. Tripal, B. Schmid, R. Palmisano, A. Mokhir, *Angew. Chem. Int. Ed.* **2018**, *57*, 11943.

- [13] H.-G. Xu, M. Schikora, M. Sisa, S. Daum, I. Klemt, C. Janko, C. Alexiou, G. Bila, R. Bilyy, W. Gong, M. Schmitt, L. Sellner, A. Mokhir, *Angew. Chem. Int. Ed.* **2021**, *60*, 11158.
- [14] S. Daum, V. Reshetnikov, M. Sisa, T. Dumych, M. D. Lootsik, R. Bilyy, E. Bila, C. Janko, C. Alexiou, M. Herrmann, L. Sellner, A. Mokhir, *Angew. Chem. Int. Ed.* **2017**, *56*, 15545.
- [15] G. Zeh, P. Haines, M. E. Miehl, T. Kienz, A. Neidlinger, R. P. Friedrich, H. G. Özkan, C. Alexiou, F. Hampel, D. M. Guldi, K. Meyer, J. Schatz, K. Heinze, A. Mokhir, *Organometallics* **2020**, *39*, 3112.
- [16] H. G. Özkan, V. Thakor, H. Xu, G. Bila, R. Bilyy, D. Bida, M. Böttcher, D. Mougiakakos, R. Tietze, A. Mokhir, *Chem. Eur. J.* **2022**, *28*, e202104420.
- [17] I. Klemt, V. Reshetnikov, S. Dutta, G. Bila, R. Bilyy, I. Cossío Cuartero, A. Hidalgo, A. Wünsche, M. Böhm, M. Wondrak, L. Kunz-Schughart, R. Tietze, F. Beierlein, P. Imhof, S. Gensberger-Reigl, M. Pischetsrieder, M. Körber, T. Jost, A. Mokhir, *RSC. Med. Chem.* **2024**. DOI: 10.1039/d3md00609c.
- [18] V. Reshetnikov, A. Arkhypov, P. R. Julakanti, A. Mokhir, *Dalton Trans.* **2018**, *47*, 6679.
- [19] V. Reshetnikov, S. Daum, A. Mokhir, *Chem. Eur. J.* **2017**, *23*, 5678.
- [20] M. Monici, *Biotechn. Ann. Rev.* **2005**, *11*, 227.
- [21] S. Daum, J. Toms, V. Reshetnikov, H. G. Özkan, F. Hampel, S. Maschauer, A. Hakimioun, F. Beierlein, L. Sellner, M. Schmitt, O. Prante, A. Mokhir, *Bioconj. Chem.* **2019**, *30*, 1077.
- [22] H. G. Özkan, J. Toms, S. Maschauer, O. Prante, A. Mokhir, *Eur. J. Inorg. Chem.* **2021**, *48*, 5096.
- [23] S. Lorenz, S. Tomcin, V. Mailänder, *Microscopy and Microanal.* **2011**, *17*, 440.
- [24] W. J. Rhee, G. Bao, *Nucleic Acid Res.* **2010**, *38*, e109.
- [25] NoBiasFluors project funded by European Union. Its description can be found under <https://cordis.europa.eu/project/id/8723312019> (accessed: 28.02.2024). Doi: 10.3030/872331.
- [26] A. R. Nödling, E. M. Mills, X. Li, D. Cardella, E. J. Sayers, S. H. Wu, A. T. Jones, L. Y. P. Luk, Y.-H. Tsai, *Chem. Comm.* **2020**, *56*, 4672.
- [27] S. Daum, S. Babiy, H. Konvalova, W. Hofer, A. Shtemenko, N. Shtemenko, C. Janko, C. Alexiou, A. Mokhir, *J. Inorg. Biochem.* **2018**, *178*, 9.
- [28] V. Weigert, T. Jost, M. Hecht, I. Knippertz, L. Heinzerling, R. Fietkau, *BMC Cancer* **2020**, *20*, 775.
- [29] J. Schindelin, I. Arganda-Carreras, E. Frise, V. Kaynig, M. Longair, T. Pietzsch, S. Preibisch, C. Rueden, S. Saalfeld, B. Schmid, J.-Y. Tinevez, D. J. White, V. Hartenstein, K. Eliceiri, P. Tomancak, A. Cardona, *Nature Methods* **2012**, *9*, 676.
- [30] R. Sens, K. H. Drexhage, *J. Luminesc.* **1981**, *24*, 709.

Manuscript received: March 19, 2024

Accepted manuscript online: June 24, 2024

Version of record online: August 8, 2024